

Tomonaga-Luttinger-liquid behavior in conducting carbon nanotubes with open ends

Hideo Yoshioka ^{a,1}

^a*Department of Physics, Nara Women's University, Nara 630-8506, Japan*

Abstract

We discuss the local density of states (LDOS) of the semi-infinite conducting carbon nanotube based on the bosonization theory of one-dimensional electron systems with open boundaries. The dependences of the spatially slowly varying component of the LDOS on location, energy and temperature are investigated.

Key words: carbon nanotube; density of states; bosonization

It has been well known that one-dimensional (1D) interacting electron systems show the behaviors called as Tomonaga-Luttinger-liquid (TLL), which is characterized by separation of the charge and spin degrees of freedom, and the interaction-dependent anomalous exponents of correlation functions. Carbon nanotubes (CNs) are one of the most promising candidates where such exotic correlation effects can be observed. In fact, in the transport experiments[1,2], power-law dependences of the conductance as a function of temperature, T , and of the differential conductance as a function of bias voltage have been observed in the metal-CN junctions and in the CN-CN junctions. These results have been interpreted to be due to tunneling between the Fermi liquid (FL) and the TLL in the former (the TLL and the TLL in the latter).

In the TLL state with the boundary, the local density of states (LDOS) shows the anomalous behaviors different from that of the FL state[3]. For example, the LDOS at the edge and that at the bulk show the power-law dependence as a function of energy at $T = 0$, but the exponent of the former is different from that of the latter. We investigate the anomalies in the LDOS of the conducting CN in detail. The spatial, energy and temperature dependences of the LDOS are discussed.

¹ Corresponding author. Tel: +81-742-20-3381; fax: +81-742-20-3381; E-mail: yoshioka@phys.nara-wu.ac.jp

We treat an (N, N) armchair CN as a model of conducting CN. The bosonized Hamiltonian effective for the low energy properties of the CN with the open boundaries is written as[4], $H = \sum_{j=\rho,\sigma} \sum_{\delta=\pm} H_{j\delta}$ where $H_{j\delta} = \pi v_{j\delta N}/(8L)(\Delta N_{j\delta} + (4\nu/3)\delta_{j\rho}\delta_{\delta-})^2 - \delta_{j\rho}\delta_{\delta+}\mu\Delta N_{\rho+} + \sum_{q>0} v_{j\delta} q b_{j\delta}^\dagger(q) b_{j\delta}(q)$ with L being the length of the CN and written as $L/a = 3n + \nu$ ($\nu = 0, \pm 1$, n : integer, a : lattice spacing of a graphite sheet). Here, $\delta = +/ -$ expresses the symmetric/antisymmetric combination between the valleys of the charge/spin ($j = \rho/\sigma$) excitation, $\Delta N_{j\delta}$ is the excess number in the mode $(j\delta)$ and $[b_{j\delta}(q), b_{j'\delta'}^\dagger(q')] = \delta_{jj'}\delta_{\delta\delta'}\delta_{qq'}$. The velocities are given as $v_{\rho+N} = v_0/K_{\rho+}^2$, $v_{\rho+} = v_0/K_{\rho+}$ and $v_{j\delta N} = v_{j\delta} = v_0$ for the others where v_0 and $K_{\rho+} \equiv e^{2\varphi}$ are respectively the Fermi velocity and the parameter depending on the interaction ($K_{\rho+} = 1$ for non-interacting case and $K_{\rho+} \simeq 0.2$ for $(10,10)$ CN). In the above Hamiltonian, the shift of the chemical potential, μ , corresponding to the applied gate voltage or difference between work function of the CN and that of the substrate are introduced. The electron operator of the spin $s = \pm$ and the sublattice $p = \pm$, $a_{ps}(r)$, are written as $a_{ps}(r) = e^{iK_y^0 y} \sqrt{a/(4N)} \sum_{\alpha,\beta=\pm} \beta p^{(1+\alpha)/2} e^{i\alpha\beta K_0 x} \psi_{R\alpha s}(\beta x)$ where $K_y^0 = 2\pi/(\sqrt{3}a)$, $K_0 = 2\pi/(3a)$ and $\psi_{R\alpha s}(x) = (\eta_{\alpha s} e^{-i\theta_{\alpha s}} / \sqrt{2\pi\tilde{a}}) \exp[i\pi x/(4L)\{\Delta N_{\rho+} + \alpha(\Delta N_{\rho-} + 4\nu/3) + s\Delta N_{\sigma+} + \alpha s\Delta N_{\sigma-}\}] \exp[(i/2)\{\cosh\varphi\phi_{\rho+}(x) -$

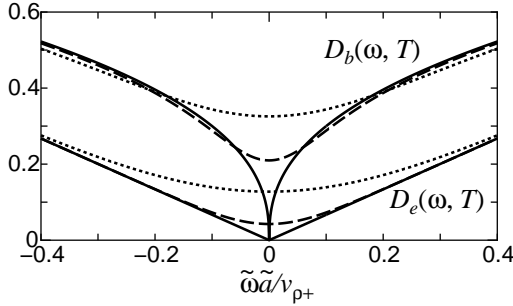


Fig. 1. The NLDOSs, $D_e(\omega, T)$ and $D_b(\omega, T)$, as a function of $\tilde{\omega}a/v_{\rho+}$ for $\pi T\tilde{a}/v_{\rho+} = 0$ (solid curve), 0.1 (dashed one) and 0.3 (dotted one).

$\sinh \varphi_{\rho+}(-x) + \alpha \phi_{\rho-}(x) + s \phi_{\sigma+}(x) + \alpha s \phi_{\sigma-}(x) \}$ with $\phi_{j\delta}(x) = \sum_{q>0} \sqrt{\pi/(qL)} \{ e^{iqx-\tilde{a}q/2} b_{j\delta}(q) + \text{h.c.} \}$ (\tilde{a} is the cut-off of the order of the radius of the tube). Here, $\{\eta_{\alpha s}, \eta_{\alpha' s'}\} = 2\delta_{\alpha\alpha'}\delta_{ss'}$, $[\theta_{\alpha s}, \Delta N_{\rho+(-)}] = i(i\alpha)$, and $[\theta_{\alpha s}, \Delta N_{\sigma+(-)}] = is(i\alpha s)$.

The LDOS given by the thermal average of $(2\pi)^{-1} \int_{-\infty}^{\infty} dt e^{i\omega t} \{ a_{ps}^\dagger(r), a_{ps}(r, t) \}$ consists of the spatially slowly varying component and the part with rapid oscillation. The former in the case of $K_{\rho+} = 1$ is a constant given by $a/(2\pi v_0 N)$. We discuss the slowly varying component normalized by the value. The dimensionless LDOS is called as the NLDOS in the following. The NLDOS is obtained for the semi-infinite case, $L \rightarrow \infty$, as $D(x, \omega, T) = v_0/(2\pi\tilde{a}) \int_{-\infty}^{\infty} dt e^{i(\omega-\mu)t} \{ u(x, t, T) + (t \rightarrow -t) \}$ where,

$$u(x, t, T) = \left[\frac{\tilde{a}h(t)}{\tilde{a} - iv_{\rho+}t} \right]^{(K_{\rho+} + K_{\rho+}^{-1})/8} \left[\frac{\tilde{a}h(t)}{\tilde{a} - iv_0t} \right]^{3/4} \times \left[\frac{\tilde{a} + i(2x - v_{\rho+}t)}{\sqrt{(2x)^2 + \tilde{a}^2}} \frac{\tilde{a} - i(2x + v_{\rho+}t)}{\sqrt{(2x)^2 + \tilde{a}^2}} \right] \times \left[\frac{h^2(2x/v_{\rho+})}{h(t + 2x/v_{\rho+})h(t - 2x/v_{\rho+})} \right]^{(K_{\rho+} - K_{\rho+}^{-1})/16}, \quad (1)$$

where $h(t) = \pi Tt/\sinh(\pi Tt)$. Thus, the center of LDOS moves as much as the shift of the chemical potential. Note that $D(x, \mu, 0) = 0$ as long as $K_{\rho+} < 1$.

At first, we consider the NLDOS at the end ($x = 0$) and the bulk position ($x = \infty$). We show $D_{e/b}(\omega, T) \equiv D(0/\infty, \omega, T)$ in Fig.1 as a function of $\tilde{\omega} = \omega - \mu$ for several choices of T , where $K_{\rho+} = 0.2$ is used. Both $D_e(\omega, 0)$ and $D_b(\omega, 0)$ show the power-law behavior as $D_j(\omega, 0) = K_{\rho+}^{1/4} (\tilde{\omega}a/v_{\rho+})^{\alpha_j} / \Gamma(\alpha_j + 1)$ where $\alpha_b = (K_{\rho+} + K_{\rho+}^{-1})/8 - 1/4$ and $\alpha_e = (K_{\rho+}^{-1} - 1)/4$. For $T > 0$, the spectral density appears at $\omega = \mu$ as $D_j(\mu, T) = K_{\rho+}^{1/4} (2\tilde{a}\pi T/v_{\rho+})^{\alpha_j} \Gamma^2((\alpha_j + 1)/2) / \Gamma(\alpha_j + 1) / \pi$.

Next we consider the case for $x \gg \tilde{a}$. The quantities, $D(x, \omega, 0)$ and $D(x, \mu, T)$, show the following scaling behaviors, $D(x, \omega, 0) = (2/\pi) K_{\rho+}^{1/4} (\tilde{a}/2x)^{\alpha_b} F(2x\tilde{\omega}/v_{\rho+})$

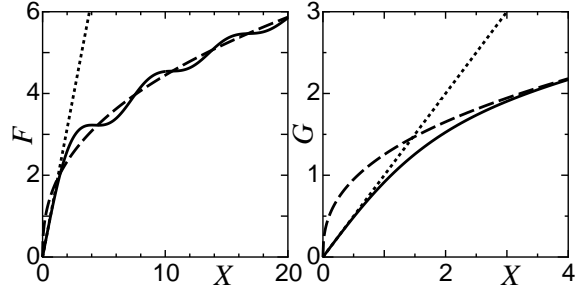


Fig. 2. Scaling functions, F and G , as a function of X . The dotted and dashed curves express the asymptotic behavior for $X \ll 1$ and $X \gg 1$, respectively.

and $D(x, \mu, T) = (2/\pi) K_{\rho+}^{1/4} (\tilde{a}/2x)^{\alpha_b} G(2\pi T x/v_{\rho+})$, where,

$$\left\{ \begin{array}{l} F(X) \\ G(X) \end{array} \right\} = -\left(\sin \frac{\pi \alpha_b}{2} \int_0^X dy + \sin \frac{\pi \alpha_e}{2} \int_X^\infty dy \right) \left\{ \begin{array}{l} f(y) \\ g(y) \end{array} \right\}, \quad (2)$$

$$f(y) = \frac{\cos y - 1}{y^{\alpha_b+1}} \frac{X^{\alpha_e}}{[(X+y)|X-y|]^{(\alpha_e-\alpha_b)/2}}, \quad (3)$$

$$g(y) = \frac{X^{\alpha_b}}{\sinh^{\alpha_b+1} y} \left[\frac{\sinh^2 X}{\sinh(X+y) \sinh(X-y)} \right]^{(\alpha_e-\alpha_b)/2} - \frac{X^{\alpha_b}}{y^{\alpha_b+1}} \left[\frac{X^2}{(X+y)|X-y|} \right]^{(\alpha_e-\alpha_b)/2}. \quad (4)$$

The scaling functions, $F(X)$ and $G(X)$, are shown in Fig.2 for $K_{\rho+} = 0.2$. Note that both $F(X)$ and $G(X)$ are proportional to X^{α_e} (X^{α_b}) for $X \ll 1$ ($X \gg 1$).

Finally, we comment on the quantitative difference between the present results and the case of the 1D Hubbard model. In the 1D Hubbard model away from half-filling, which is well understood in terms of the TLL, the bulk and end exponent do not exceed 1/8 and 1/2, respectively[3]. On the other hand, for example, the exponent in the (10,10) CN is about 0.4 for the bulk and 1.0 for the end. The larger values are due to the long range nature of the mutual interaction. In this sense, the CN is considered to be a system in which one can observe the TLL behavior well.

This work was supported by Grant-in-Aid for Encouragement of Young Scientist (No. 13740220) and for Scientific Research (A) (No. 13304026) and (C) (No. 14540302) from the Ministry of Education, Culture, Sports, Science and Technology, Japan.

References

- [1] M. Bockrath *et al.*, Nature (London) **397** (1999) 598.
- [2] Z. Yao *et al.*, Nature (London) **402** (1999) 271.
- [3] A.E. Mattsson *et al.*, Phys. Rev. B **56** (1997) 15615.
- [4] H. Yoshioka, Y. Okamura, cond-mat/0205503.